

*Advanced* 

# Synthesis & Catalysis

## Accepted Article

**Title:** Reprogramming epoxide hydrolase to improve enantioconvergence in hydrolysis of styrene oxide scaffolds

**Authors:** fulong li, Yanyan Qiu, Yucong Zheng, Feifei Chen, Xudong Kong, Jian-He Xu, and Hui-Lei Yu

This manuscript has been accepted after peer review and appears as an Accepted Article online prior to editing, proofing, and formal publication of the final Version of Record (VoR). This work is currently citable by using the Digital Object Identifier (DOI) given below. The VoR will be published online in Early View as soon as possible and may be different to this Accepted Article as a result of editing. Readers should obtain the VoR from the journal website shown below when it is published to ensure accuracy of information. The authors are responsible for the content of this Accepted Article.

**To be cited as:** *Adv. Synth. Catal.* 10.1002/adsc.202000898

**Link to VoR:** <https://doi.org/10.1002/adsc.202000898>

DOI: 10.1002/adsc.202((will be filled in by the editorial staff))

# Reprogramming Epoxide Hydrolase to Improve Enantioconvergence in Hydrolysis of Styrene Oxide Scaffolds

Fu-Long Li, Yan-Yan Qiu, Yu-Cong Zheng, Fei-Fei Chen, Xu-Dong Kong, Jian-He Xu\* and Hui-Lei Yu\*

State Key Laboratory of Bioreactor Engineering, Shanghai Collaborative Innovation Centre for Biomanufacturing and Frontiers Science Center for Materiobiology and Dynamic Chemistry, East China University of Science and Technology, Shanghai 200237, China. Fax: (+86)-21-6425-0840, Email: jianhexu@ecust.edu.cn; huileiyu@ecust.edu.cn.

Received: ((will be filled in by the editorial staff))

Supporting information for this article is available on the WWW under <http://dx.doi.org/10.1002/adsc.201#####>. ((Please delete if not appropriate))

**Abstract.** Enantioconvergent hydrolysis by epoxide hydrolase is a promising method for the synthesis of important vicinal diols. However, the poor regioselectivity of the naturally occurring enzymes results in low enantioconvergence in the enzymatic hydrolysis of styrene oxides. Herein, modulated residue No. 263 was redesigned based on structural information and a smart variant library was constructed by site-directed modification using an “optimized amino acid alphabet” to improve the regioselectivity of epoxide hydrolase from *Vigna radiata* (VrEH2). The regioselectivity coefficient ( $r$ ) of variant M263Q for the *R*-isomer of *meta*-substituted styrene oxides was improved 40–63-fold, and variant M263V also exhibited higher regioselectivity towards the *R*-isomer of *para*-substituted styrene oxides compared with the wild type, which resulted in improved enantioconvergence in hydrolysis of styrene oxide scaffolds. Structural insight showed the crucial role of residue No. 263 in modulating the substrate binding conformation by altering the binding surroundings. Furthermore, increased differences in the attacking distance between nucleophilic residue Asp101 and the two carbon atoms of the epoxide ring provided evidence for improved regioselectivity. Several high-value vicinal diols were readily synthesized (>88% yield, 90%–98% *ee*) by enantioconvergent hydrolysis using the reprogrammed variants. These findings provide a successful strategy for enhancing the enantioconvergence of native epoxide hydrolases through key single-site mutation and more powerful enzyme tools for the enantioconvergent hydrolysis of styrene oxide scaffolds into single (*R*)-enantiomers of chiral vicinal diols.

**Keywords:** epoxide hydrolase; enantioconvergent hydrolysis; regioselectivity; structural re-designing; vicinal diols

## Introduction

Chiral vicinal diols and epoxides are ubiquitous synthons for the preparation of versatile  $\beta$ -adrenergic receptor agonist ( $\beta$ -blocker) drugs and amino alcohols.<sup>[1]</sup> Much effort has been devoted to exploring efficient approaches for the synthesis of chiral vicinal diols and epoxides.<sup>[2]</sup> Biocatalytic strategies can provide environmentally friendly options, as exemplified by the asymmetric reduction of hydroxyketone using oxidoreductase. However, oxidoreductases require expensive coenzymes and lack the desired activity.<sup>[3]</sup> As an alternative route, the hydrolysis of racemic epoxides using cofactor-independent epoxide hydrolases (EHs) shows great promise for the synthesis of chiral vicinal diols. This can be conducted using either kinetic resolution or enantioconvergent hydrolysis.<sup>[4]</sup> Enantioconvergent hydrolysis can simultaneously catalyse pairs of epoxide enantiomers with complementary

regioference, forming an enantioenriched product with a 100% theoretical yield.<sup>[5]</sup> As regioselectivity is a key determinant of enantioconvergence, regioselectivity coefficients ( $\alpha$  and  $\beta$ ), are used to quantify the degree of regioselectivity, indicating the attack percentages at carbon atoms  $C_\alpha$  and  $C_\beta$  of an epoxide enantiomer (either *R*- or *S*-configuration), respectively.<sup>[6]</sup>

Owing to the uniqueness and importance of enantioconvergent hydrolysis in chiral synthesis, a few enantioconvergent EHs from plants and microbes have been discovered and characterized in recent decades.<sup>[6,7]</sup> These enzymes can completely hydrolyse the two enantiomers of a racemic epoxide into enantioenriched chiral vicinal diols. However, naturally occurring EHs generally suffer from insufficient regioselectivity towards both enantiomers of epoxide substrates, resulting in incomplete enantioconvergence. Protein engineers aim to evolve the performance of enzymes in terms of regio- or enantioselectivity.<sup>[8]</sup> For example, the regioselectivity factors ( $\alpha_R$ ,  $\alpha_S$ ) of engineered *Kau 2* EH were

improved by 17% and 87% toward (*S*)- and (*R*)-enantiomers of *para*-chlorostyrene oxide, respectively.<sup>[9]</sup> Furthermore, a three-site mutant of PvEH1 also exhibited higher regioselectivity ( $\alpha_R = 86\%$ ,  $\alpha_S = 99\%$ ) than the wild-type toward styrene oxide.<sup>[7f]</sup>

In our previous study, a novel epoxide hydrolase (*VrEH*<sub>2</sub>) discovered from *Vigna radiata* was shown to enantioconvergently hydrolyse racemic *para*-nitrostyrene oxide (*rac*-pNSO).<sup>[7a,7b]</sup> However, unsatisfactory regioselectivity and strict substrate specificity severely limited its application scope. Subsequently, a semi-rational design strategy was adopted that revealed a crucial residue (Met263) for precise modulation of the regioselectivity.<sup>[10]</sup> This resulted in near-perfect enantioconvergence toward *rac*-pNSO after single-site mutation (M263N). However, the enantioconvergence of *VrEH*<sub>2</sub> must be improved for the enzymatic hydrolysis of other styrene oxides with different substitution groups. Recently, a variant of PvEH1 was obtained by reshaping its two substrate tunnels, exhibiting enhanced enantioconvergence towards *meta*-chlorostyrene oxide (>99% conversion, 95.6% *ee*).<sup>[11]</sup> However, examples of perfect enantioconvergence (>99% conversion, >99% *ee*) towards other substituted styrene oxide have yet to be reported, which severely limits the catalytic application of EHs in the synthesis of important chiral intermediates.

Herein, to explore the enantioconvergent potential of *VrEH*<sub>2</sub> in the biohydrolysis of various epoxide scaffolds, a smart mutant library was constructed by redesigning the enzyme based on the previously identified key site. The resultant variants showed enhanced enantioconvergence towards a series of styrene oxides. More importantly, the regioselectivity modulation mechanism for differently substituted styrene oxides was elucidated based on structural information from variants and docking results. This will aid the design of additional and improved enantioconvergent EHs for the green and efficient synthesis of high-value vicinal diols.

## Results and Discussion

### Constructing a smart mutant library by reprogramming regioselectivity modulating residue Met263

The crucial regioselectivity modulating residue, Met263 of *VrEH*<sub>2</sub>, was identified previously by structure-guided semi-rational design (**Figure 1**). Mutations on this site significantly modulated the enantioconvergence of *VrEH*<sub>2</sub> toward *rac*-pNSO. The polar side chain of Asn263 from the M263Q mutation formed a new hydrogen bond with the *para*-nitro group of pNSO, enabling a clear shift in substrate binding pose that led to improved regioselectivity. In

contrast, mutating to Phe or Trp with bulky sidechains caused a severe decrease in regioselectivity. Herein, to rationally and efficiently construct variants for improved enantioconvergence towards other styrene oxide scaffolds, an “optimized amino acid alphabet” consisting of six pre-selected residues (Ala-Val-Ser-Cys-Asn-Gln) was designed in accordance with CAST (Combinatorial Active-site Saturation Test) method and the previous studies.<sup>[12]</sup> A smart mutant library on the key residue (Met263) was then constructed by site-directed mutagenesis using the simplified amino acid alphabet.

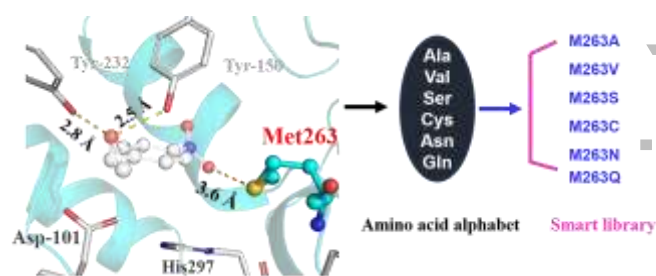


**Figure 1.** Structural insight of the key residue (Met-263) locating in the active centre, the optimized amino acid alphabet for constructing a smart library was indicated. The catalytic residue Asp101 oxyanion hole residues (Tyr150 and Tyr232) were shown in grey.

To verify the enantioconvergence of the redesigned variants in the hydrolysis of epoxide scaffolds, substrates **1a–17a** bearing different substituents were designed (**Scheme S1, Figure 2**) and the enantiomeric excess (*ee*) of the corresponding vicinal diols was determined (**Figure S1**). For styrene oxide (**1a**), *para*-substituted **2a–6a**, and *ortho*-substituted **12a**, the wild type (WT) showed partial enantioconvergence, with *ee*<sub>p</sub> values of 60%–93%. Meanwhile, poor *ee*<sub>p</sub> values of 8%–21% were obtained for *meta*-substituted substrates **8a–11a**, except for the fluorinated compound **7a**, clearly indicating that the position and properties of the substituent group on the benzene ring affected enantioconvergence using the EHs. The *ee*<sub>p</sub> values for *para*- and *meta*-disubstituted substrates **13a** and **14a** were clearly lower than those of *para*-monosubstituted substrates **2a** and **3a**, indicating that the additional *meta*-substituent significantly influenced product selectivity. The *ee*<sub>p</sub> values of *para*- and *ortho*-disubstituted epoxides **15a** and **16a** were similar to those of *para*-monosubstituted substrates **2a** and **3a**, suggesting that an additional *ortho*-substituent did not affect the regioselectivity.

Among the redesigned variants, M263Q, M263V, and M263N showed significantly improved enantioconvergence towards a series of styrene oxides. For *para*- and nonsubstituted substrates **1a–**

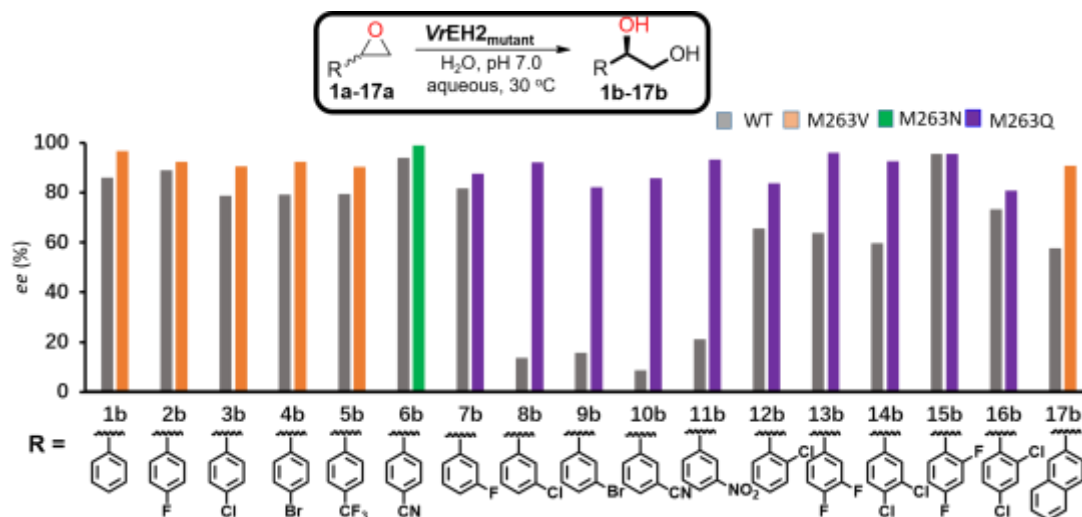


**Figure 2.** The *ee* values of product (**1b-17b**) by entioconvergent hydrolysis of substrate **1a-17a** using WT and variants M263Q, M263V or M263N.

**Table 1** The regioselectivities of WT and variant M263Q towards two enantiomers of *meta*-substituted styrene oxides **8a-11a**.

Substrate	Enzyme	$\alpha$ (%) <sup>a</sup>	$\beta$ (%) <sup>a</sup>	$r$ <sup>b</sup>	Fold ( $r$ )
<i>(R)</i> - <b>8a</b>	WT	75 ± 0.0	25 ± 0.0	0.3	--
	M236Q	7 ± 0.0	93 ± 0.0	13	<b>43</b>
<i>(S)</i> - <b>8a</b>	WT	85 ± 0.1	15 ± 0.1	5.7	--
	M236Q	98 ± 0.0	2 ± 0.0	49	<b>8.5</b>
<i>(R)</i> - <b>9a</b>	WT	73 ± 0.4	27 ± 0.4	0.3	--
	M236Q	5 ± 0.1	95 ± 0.1	19	<b>63</b>
<i>(S)</i> - <b>9a</b>	WT	90 ± 0.7	10 ± 0.7	9	--
	M236Q	95 ± 0.2	5 ± 0.2	19	<b>2.1</b>
<i>(R)</i> - <b>10a</b>	WT	81 ± 0.3	19 ± 0.3	0.2	--
	M236Q	8 ± 0.2	92 ± 0.2	11	<b>55</b>
<i>(S)</i> - <b>10a</b>	WT	64 ± 0.3	36 ± 0.3	1.8	-
	M236Q	90 ± 0.2	10 ± 0.2	9	<b>5</b>
<i>(R)</i> - <b>11a</b>	WT	62 ± 0.1	38 ± 0.1	0.6	--
	M263Q	4 ± 0.5	96 ± 0.5	24	<b>40</b>
<i>(S)</i> - <b>11a</b>	WT	77 ± 0.3	23 ± 0.3	3.3	--
	M263Q	94 ± 0.0	6 ± 0.0	15	<b>4.5</b>

<sup>a</sup>  $\alpha$ ,  $\beta$  (%) are regioselectivity coefficients indicating the attacking percentage of the C $\alpha$  and C $\beta$  of (*S*)-enantiomers or (*R*)-enantiomers, respectively.

<sup>b</sup>  $r$  (regioselectivity ratio) is calculated as  $\alpha/\beta$  (*S*) or  $\beta/\alpha$  (*R*), which represents the specificity of the regioselectivity attacking.

**5a** and bulky substrate **17a**, variant M263V showed better enantioconvergence, with a higher *ee<sub>p</sub>* value (90%) than that of WT (*ee<sub>p</sub>*, 57%–79%). In particular, M263N was found to exhibit near-perfect enantioconvergence toward *rac*-**6a**, with the *ee* value of **6b** improved to 99% (*ee<sub>p</sub>* of WT = 93%). The enantioconvergence of M263Q towards *meta*-substituted styrene oxides **8a-10a** increased significantly, and the optical purities of **8b** and **11b**

were more than 92% (**Figure 2**). Furthermore, the enantioconvergence of M263Q towards **7a** and **12a-16a** was improved by an *ee<sub>p</sub>* value of 80%–95%. These results indicated that redesigning the residue (M263) engineered enantioconvergence of VrEH2 towards a series of substituted styrene oxides, which significantly expanded the substrate scope of VrEH2 in an entioconvergent manner.

### Determination of regioselectivities toward *para*- and *meta*-substituted styrene oxides to characterize the improved enantioconvergence

To characterize the improved enantioconvergence of M263V and M263Q, the regioselectivity ratios ( $r$ ) towards *para*- and *meta*-substituted styrene oxides were measured using optically pure (*S*)- or (*R*)-epoxides as substrates, respectively. The regioselectivity ratio ( $r$ ) indicated the difference in the enzyme attacking frequencies at  $C\alpha$  and  $C\beta$  of the epoxide ring, and was calculated experimentally by measuring the molar ratio of diol isomers obtained using an optically pure substrate.<sup>29</sup> As shown in **Table S1**, both WT and M263V showed high  $r_S$  values of more than 49.0 for the *S*-enantiomer of *para*-substituted substrates **1a**, **3a**, and **4a**, while the  $r_R$  values of the wild-type for **1a**, **3a**, and **4a** were only 5.6, 4.3, and 3.5, respectively. Therefore, the insufficient regioselectivity of WT toward *R*-enantiomers **1a**, **3a**, and **4a** was the main origin of low enantioconvergence. Comparatively, the  $r_R$  value of variant M263V toward (*R*)-**1a** reached 32.3, representing a 5.8-fold increase compared with the WT, and the original regioselectivity toward (*S*)-**1a** ( $r_S = 49.0$ ) was retained, causing an obvious improvement of enantioconvergence. Furthermore, the regioselectivity enhancement of variant M263V toward (*R*)-enantiomers of substrates **3a** and **4a** also led to improved enantioconvergence.

For *meta*-substituted styrene oxides **8a–11a**, the WT did not show a complementary regiopreference toward either enantiomer, and the  $r$  values toward both enantiomers were insufficient. Particularly for **8a**, **9a**, **10a**, and **11a**, the  $r_R$  values were less than 1.0 owing to the poor optical purity of product (8%–21%  $ee_p$ ). Compared with the WT, the regioselectivity of variant M263Q toward both enantiomers of substrates **8a**, **9a**, **10a**, and **11a** was improved (**Table 1**). The  $r_R$  values showed a 40–53-fold improvement towards the *R*-enantiomer and afforded the complementary regiopreference towards the *S*-enantiomer, greatly enhancing enantioconvergence in the hydrolysis of *meta*-substituted styrene oxides.

### Structural evidence for origin of improved regioselectivity

To further explore the origin of improved regioselectivity toward *para*- or *meta*-substituted styrene oxides, the crystal structures of variants M263Q (PDB ID: **7CG6**) and M263V (PDB ID: **7CG2**) were both determined at a resolution of 2.0 Å (**Table S4**). For variants M263V and M263Q, the introduction of Val263 provided a smaller side chain on the modulated site (**Figure S3A**), while the Gln263 amides group showed an inverted orientation and shifted towards catalytic residue Asp101 (**Figure S3B**). These changes caused by the mutation at Met263 would greatly affect substrate binding. Binding conformations with the WT and variants

were also simulated for *para*- or *meta*-substituted styrene oxide substrates (*R*)-**3a** and (*R*)-**8a** (**Figure 3**). For WT, the epoxide ring of (*R*)-**3a** and (*R*)-**8a** was positioned between the catalytic residue (Asp101) and oxygen hole residues (Tyr150, Tyr232). Furthermore, the geometric distances between Asp101 and the  $C\alpha$  ( $d_{C\alpha}$ ) or  $C\beta$  ( $d_{C\beta}$ ) atoms of the epoxide ring were both less than 3.5 Å, with distance differences ( $\Delta d$ ) of only 0.2 Å. This indicated the two positions could be equally attacked by catalytic residue, which was consistent with the regioselectivity coefficients detected experimentally. For M263V and M263Q, the distance difference between Asp101 and the two carbons of the epoxide ring was more than 0.8 Å, and the geometric distance ( $d_{C\beta} < d_{C\alpha}$ ) indicated that  $C\beta$  was more readily attacked compared with WT.

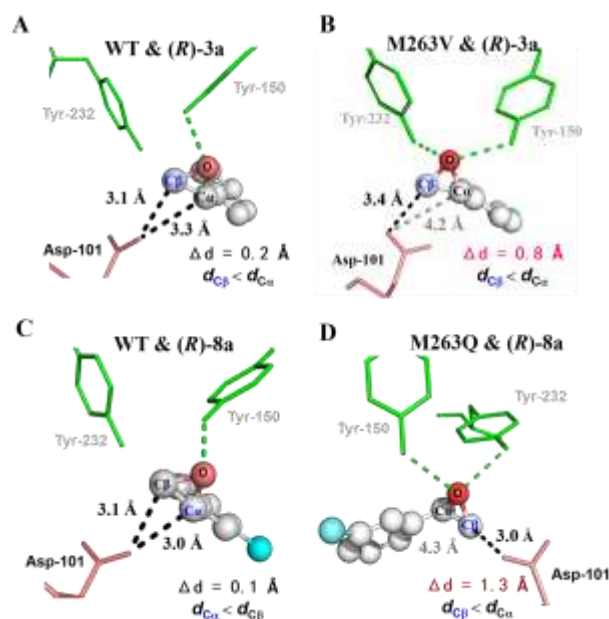


**Figure 3.** The preferred substrate binding conformations of (*R*)-**3a** and (*R*)-**8a** with WT and variants. The distances between the two carbon atoms ( $C\alpha$  and  $C\beta$ ) of epoxide ring and the nucleophile residue Asp101 were labelled.

Through structural observation, the introduction of Val263 with a smaller side chain provided a larger hydrophobic pocket. The change in binding surroundings was more beneficial to the hydrophobic *para*-substituted styrene oxide binding in a more favourable conformation from analysis of the binding energy (−4.93 kcal/mol). Furthermore, the precisely modulated conformation with the increased distance difference consolidated the attacking preference at the  $C\beta$  atom of the epoxide ring, leading to improved regioselectivity. For *meta*-substituted styrene oxide, the  $C\alpha$  atom of the epoxide ring was readily attacked in the WT binding conformation, which was undesirable regarding distance difference. In contrast, substituting Met263 into residues Gln263 with a polar side chain significantly changed the original binding environment, resulting in a substrate binding pose in

the opposite orientation compared with that of the WT (**Figure S4**). The geometric distance between Asp101 and the C $\alpha$  ( $d_{C\alpha}$ ) or C $\beta$  ( $d_{C\beta}$ ) atoms of the epoxide ring indicated that the attacking preference reversed on C $\beta$  of epoxide ring, which greatly improved its regioselectivity towards C $\beta$ . These findings verified the importance of residue 263 in modulating the epoxide binding pose by altering the binding surroundings, and a single mutation at this site could achieve the improved enantioconvergence of VrEH2 in the hydrolysis of various styrene oxides with different substituted groups or bulky substrates.

### Preparation of chiral vicinal diols via enantioconvergent hydrolysis of styrene oxides

Subsequently, to explore the potential of the redesigned enzymes in the biopharmaceuticals field, several vicinal diol products derived from substrates **1a**, **3a**, **6a**, **8a**, **13a**, **14a**, and **17a**, which are important blocks for the preparation of  $\beta$ -blocker drugs<sup>[13]</sup>, such as denopamine, FAAH inhibitors, solabegron, dichlorolsoproterenol, and pronethalol, were prepared in an enantioconvergent manner. Then a 10-mL preparative scale reaction was performed, to minimize the effect of epoxides spontaneous hydrolysis, a fed-batch mode (5 $\times$ 20 mM) was applied in the system. The results of these reactions are shown in **Table 2**. The enantioenriched vicinal diols can be prepared with high isolated yields (>88%) and high *ee* values (90%-98%), and the final optical purity of some products can be further improved by recrystallized method<sup>[7a]</sup>. Compared to current pathways using metal catalysts or (salen) CoIII complexes,<sup>[14]</sup> the enantioconvergent manner provides a promising and green pathway for the synthesis of pharmaceutically relevant chiral diols.

**Table 2.** Enzymatic synthesis of (*R*)-vicinal diols by enantioconvergent hydrolysis of styrene oxides.<sup>a</sup>

Substrate	Enzyme	Time (h)	Isolated yield	<i>ee</i> <sub>p</sub> (%)	STY (g·L <sup>-1</sup> ·d <sup>-1</sup> )
<i>rac</i> - <b>1a</b>	M263V	1.5	90	94	199
<i>rac</i> - <b>3a</b>	M263V	3.0	91	90	126
<i>rac</i> - <b>6a</b>	M263N	5.0	92	98	72.0
<i>rac</i> - <b>8a</b>	M263Q	4.5	90	90	74.5
<i>rac</i> - <b>13a</b>	M263Q	7.5	89	90	58.3
<i>rac</i> - <b>14a</b>	M263Q	2.5	88	92	148.7
<i>rac</i> - <b>17a</b>	M263V	12.0	89	90	33.5

<sup>a</sup>The reactions were performed, including (5 $\times$ 20 mM) substrates and catalyst (20 g cdw/L), in aqueous phase system (10 mL) consisting of potassium phosphate buffer

(9 mL, pH 7.0, 100 mM) and 10% cosolvent dimethyl sulphoxide at 30 °C with stirring (400 r/min). To minimize the spontaneous hydrolysis, substrate was added by 5 batches. All the reaction processes were monitored by detecting the substrate with TLC, and the final vicinal diol products were extracted with ethyl acetate and purified by flash chromatography.

## Conclusion

Redesigning a key residue of VrEH2 resulted in a smart mutant library that produced a marked improvement in the enantioconvergent hydrolysis of structurally diverse styrene oxides. More efficient catalytic tools for chiral vicinal diols synthesis were also obtained. Structural analysis showed the crucial role of residue 263 in modulating the epoxide binding pose by precisely altering the substrate binding environment. Furthermore, the increased difference in attacking distances provided evidence to explain the improved regioselectivity. More significantly, these findings can be introduced into other homologous enzyme families to further enhance their applicability to the enantioconvergent hydrolysis of various epoxides.

## Experimental Section

### Biological and chemical reagents

Racemic substrates **1a-5a** and enantiopure (*R*)-**1a** and (*S*)-**1a** were purchased from commercial companies, while **6a-17a** were prepared according to chemical methods.<sup>8</sup> The enantiopure **3a**, **4a**, **8a**, **9a**, **11a**, **12a** were obtained by preparative HPLC (Shanghai Chiralway Biotech Co., Ltd, China). All designed oligonucleotide primers were prepared by SangonTech (Shanghai, China). The *E. coli* BL21 (DE3) were used for expression of protein. All used restriction enzymes and biological reagents of molecular experiment were purchased from New England Biolabs (Beijing, China).

### Site-directed Mutagenesis

Mutants were constructed by site-directed mutagenesis *via* PCR using PrimeSTAR. The site-directed primers (**Table S1**) were designed by software NewDNA. Nearly 100 ng recombinant plasmid pET28-VrEH2 was used as template and the PCR was performed according to the general procedures. After digestion by endonuclease *Dpn* I, the PCR product was transformed into *E. coli* BL21 (DE3). All the resulting mutants were verified by sequence analysis.

### Expression and purification of variants

The recombinant cells were grown in Luria-Bertani medium containing 50  $\mu$ g/mL kanamycin for nearly 2.5-3 h in a shaker under 37 °C and 180 rpm. The inducer IPTG was added with a final concentration of 0.2 mM when the OD<sub>600</sub> value of the growing cell reached 0.6-0.8. The cells

Accepted Manuscript

were induced for expression of the aimed protein for 24 h under 16 °C and 180 rpm. The lysis buffer (20 mM Tri-HCl buffer, 300 mM NaCl and 20 mM imidazole, 5 mM  $\beta$ -mercaptoethanol, pH 8.0) was prepared for cells re-suspending. After sonication disruption, the cell lysate was centrifuged for 50 min (10,956 g) under 4 °C to obtain supernatant. The cell free extract was purified by HisTrap Ni<sup>+</sup> affinity column (GE-healthcare) as described previously.<sup>[10]</sup>

### Regioselectivity coefficient assay

Using optically pure (*S*)- or (*R*)-epoxides as substrates, the configuration of products was determined by the attacking preference of the enzyme on the two carbon atoms of epoxide ring (regioselectivity).<sup>[15]</sup> Thus the regioselectivity coefficients can be deduced by calculating molar ratio of the two enantiomers of product in hydrolysis of enantiopure epoxides. Enantiopure substrate (10 mM, 50  $\mu$ L) was added to potassium phosphate buffer (100 mM, pH 7.0, 450  $\mu$ L) containing purified enzyme (0.1 mg/mL) and the reaction mixture was agitated at 30 °C and 1000 rpm. Then the reaction mixture was extracted by an equal volume of ethyl acetate when the reaction was converted completely. The molar ratio of the two enantiomers of product was analyzed by HPLC (Shimadzu LC-10AT) with a chiral OD-H column (Daicel, 4.6  $\Phi$   $\times$  250 mm).

### Preparing chiral vicinal diols by enzymatic enantioconvergent hydrolysis of styrene oxides

A representative enantioconvergent hydrolysis reaction was carried out in a 10-mL reaction system. The recombinant *E.coli* cells were re-suspended in buffer (pH 7.0, 100 mM potassium phosphate, containing 10% (v/v) dimethyl sulfoxide) at a final concentration of 15 g cdw/L (cdw = dry cell weight), the substrate (0.02 mol) was fed by 5 batches and the total substrate loading reached 100 mM. The reaction was performed in a stirring reactor under 30 °C and 400 r/min and the reaction process were monitored by TLC. When the substrate was totally converted, the product was extracted using ethyl acetate (5  $\times$  10 mL). The combined organic phase was washed with saturated NaCl solution (2  $\times$  50 mL), then dried over anhydrous Na<sub>2</sub>SO<sub>4</sub> for 12 h, then concentrated under reduced pressure. The resulting residual was purified by flash chromatography on silica gel eluted with petroleum ether/ethyl acetate. <sup>1</sup>H and <sup>13</sup>C NMR data and optical rotation of the vicinal diols were listed as following:

**(R)-1-Phenyl-1,2-ethanediol (1b):** white solid; 124 mg, yield 90%; 94% *ee*. [ $\alpha$ ]<sub>D</sub><sup>30</sup>: -40.0 (*c* 1.0, EtOH). lit.<sup>[16]</sup>. [ $\alpha$ ]<sub>D</sub><sup>25</sup>: -37.8 (*c* 1.0, EtOH). <sup>1</sup>H NMR (400 MHz, CDCl<sub>3</sub>)  $\delta$  7.37 (d, *J* = 4.4 Hz, 4H), 7.34-7.29 (m, 1H), 4.83 (dd, *J* = 8.2, 3.5 Hz, 1H), 3.77 (dd, *J* = 11.3, 3.5 Hz, 1H), 3.67 (dd, *J* = 11.3, 8.2 Hz, 1H), 2.21 (br, 2H). <sup>13</sup>C NMR (150 MHz, CDCl<sub>3</sub>)  $\delta$  140.4, 128.5, 127.9, 126.1, 74.7, 68.0.

**(R)-1-(4-Chlorophenyl)-1,2-ethanediol (3b):** white solid; 157 mg, yield 91%; 90% *ee*. [ $\alpha$ ]<sub>D</sub><sup>30</sup>: -64.0 (*c* 1.0, CHCl<sub>3</sub>). lit.<sup>[16]</sup>. [ $\alpha$ ]<sub>D</sub><sup>25</sup>: -55.9 (*c* 1.0, CHCl<sub>3</sub>). <sup>1</sup>H NMR (400 MHz, CDCl<sub>3</sub>)  $\delta$  7.37-7.28 (m, 4H), 4.80 (dd, *J* = 8.1, 3.3 Hz, 1H), 3.75 (dd, *J* = 11.3, 3.3 Hz, 1H), 3.61 (dd, *J* = 11.2, 8.2 Hz, 1H),

2.36 (br, 2H). <sup>13</sup>C NMR (150 MHz, DMSO-*d*<sub>6</sub>)  $\delta$  143.0, 131.7, 128.6, 128.2, 73.5, 67.65.

**(R)-1-(4-Cyanophenyl)-1,2-ethanediol (6b):** white solid; 150 mg, yield 92%; 98% *ee*. [ $\alpha$ ]<sub>D</sub><sup>30</sup>: -24.0 (*c* 1.0, EtOH). lit.<sup>[17]</sup>. [ $\alpha$ ]<sub>D</sub><sup>25</sup>: -20.5 (*c* 0.8, EtOH). <sup>1</sup>H NMR (400 MHz, CDCl<sub>3</sub>)  $\delta$  7.69-7.62 (m, 2H), 7.51 (d, *J* = 8.1 Hz, 2H), 4.89 (dd, *J* = 8.0, 3.4 Hz, 1H), 3.81 (dd, *J* = 11.2, 3.5 Hz, 1H), 3.62 (dd, *J* = 11.2, 8.0 Hz, 1H), 2.34 (br, 2H). <sup>13</sup>C NMR (150 MHz, DMSO-*d*<sub>6</sub>)  $\delta$  140.9, 136.2, 128.9, 126.7, 74.2, 68.0, 21.2.

**(R)-1-(3-Chlorophenyl)-1,2-ethanediol (8b):** colorless oil; 155 mg, yield 90%; 90% *ee*. [ $\alpha$ ]<sub>D</sub><sup>25</sup>: -26.0 (*c* 1.0, EtOH). lit.<sup>[16]</sup>. [ $\alpha$ ]<sub>D</sub><sup>25</sup>: -22.5 (*c* 1.1, EtOH). <sup>1</sup>H NMR (400 MHz, CDCl<sub>3</sub>)  $\delta$  7.32 (s, 1H), 7.27-7.23 (m, 2H), 7.16 (dd, *J* = 6.3, 2.3 Hz, 1H), 4.72 (dd, *J* = 8.3, 3.2 Hz, 1H), 3.68 (dd, *J* = 11.5, 3.3 Hz, 1H), 3.63 (s, 2H), 3.55 (dd, *J* = 11.6, 8.4 Hz, 1H). <sup>13</sup>C NMR (100 MHz, CDCl<sub>3</sub>)  $\delta$  151.5 (dd, *J* = 49.0, 12.7 Hz, 1C), 149.0 (dd, *J* = 49.0, 12.7 Hz, 1C), 137.6 (dd, *J* = 5.0, 3.9 Hz, 1C), 122.0 (dd, *J* = 6.4, 3.7 Hz, 1C), 117.3 (d, *J* = 17.3 Hz, 1C), 115.1 (d, *J* = 17.9 Hz, 1C), 73.5, 67.8.

**(R)-1-(3,4-Fluorophenyl)-1,2-ethanediol (13b):** colorless oil; 155 mg, yield 89%; 92% *ee*. [ $\alpha$ ]<sub>D</sub><sup>25</sup>: -38.0 (*c* 1.0, EtOH). <sup>1</sup>H NMR (400 MHz, CDCl<sub>3</sub>)  $\delta$  7.26 – 7.05 (m, 3H), 4.79 (dd, *J* = 8.1, 3.4 Hz, 1H), 3.75 (dd, *J* = 11.3, 3.5 Hz, 1H), 3.60 (dd, *J* = 11.3, 8.1 Hz, 1H), 2.22 (br, 2H). <sup>13</sup>C NMR (100 MHz, CDCl<sub>3</sub>)  $\delta$  151.4 (dd, *J* = 49.1, 12.7 Hz, 1C), 148.9 (dd, *J* = 48.8, 12.7 Hz, 1C), 139.8 – 135.0 (m, 1C), 122.0 (dd, *J* = 6.4, 3.7 Hz, 1C), 117.3 (d, *J* = 17.3 Hz, 1C), 115.12 (d, *J* = 17.9 Hz, 1C), 73.5, 67.8.

**(R)-1-(3,4-Dichlorophenyl)-1,2-ethanediol (14b):** white solid; 182 mg, yield 88%; 90% *ee*. [ $\alpha$ ]<sub>D</sub><sup>30</sup>: -40.0 (*c* 1.0, CHCl<sub>3</sub>). <sup>1</sup>H NMR (400 MHz, CDCl<sub>3</sub>)  $\delta$  7.49 (d, *J* = 1.9 Hz, 1H), 7.46-7.39 (m, 1H), 7.20 (dd, *J* = 8.3, 1.9 Hz, 1H), 4.80 (dd, *J* = 8.0, 3.4 Hz, 1H), 3.77 (dd, *J* = 11.2, 3.5 Hz, 1H), 3.61 (dd, *J* = 11.2, 8.0 Hz, 1H), 2.14 (br, 2H). <sup>13</sup>C NMR (150 MHz, DMSO-*d*<sub>6</sub>)  $\delta$  145.3, 131.0, 130.4, 129.6, 128.8, 127.2, 72.9, 67.3.

**(R)-1-(2-Naphthalenyl)-1,2-ethanediol (17b):** white solid; 167.5 mg, yield 89%; 90% *ee*. [ $\alpha$ ]<sub>D</sub><sup>30</sup>: -32.0 (*c* 1.0, EtOH). lit.<sup>[17]</sup>. [ $\alpha$ ]<sub>D</sub><sup>25</sup>: -28.6 (*c* 0.79, EtOH). <sup>1</sup>H NMR (400 MHz, DMSO-*d*<sub>6</sub>)  $\delta$  7.93-7.82 (m, 4H), 7.49 (tdd, *J* = 9.0, 5.8, 3.4 Hz, 3H), 5.38 (d, *J* = 4.2 Hz, 1H), 4.77 (t, *J* = 5.8 Hz, 1H), 4.71 (dd, *J* = 10.3, 5.8 Hz, 1H), 3.53 (t, *J* = 5.9 Hz, 2H). <sup>13</sup>C NMR (150 MHz, DMSO-*d*<sub>6</sub>)  $\delta$  141.6, 133.3, 132.8, 128.2, 127.9, 127.7, 126.4, 125.9, 125.5, 125.2, 74.4, 67.8.

### Crystallization, structure determination and molecular docking

After Ni<sup>+</sup> column purification, the collected protein was further purified using a gel filtration column (Superdex 75 Hiload 16/60) to obtain protein as monomer in solution. Protein samples (VrEH2<sub>M263Q</sub> 16 mg/mL, VrEH2<sub>M263V</sub> 18 mg/mL) were added in 96 well sitting-drop plate and mixed with equal volume (2  $\mu$ L) of crystallization solution. The crystal growing condition (0.15 M Tris-HCl, pH 8.5, 35% PEG3350, 18 °C) of VrEH2<sub>M263Q</sub> and VrEH2<sub>M263V</sub> were same as wild type, protein crystals could be observed in diamond shaped after three days. Crystals were flash-cooled with liquid nitrogen in crystallization solution containing 10% (v/v) glycerol as cryoprotectant and used

for X-ray diffraction. The diffraction data of crystals were collected at beamline BL17U1 of the Shanghai Synchrotron Radiation Facility (SSRF),<sup>[18]</sup> and the software HKL2000 was used for data indexing, integrating and scaling.<sup>[19]</sup> The initial structure model of mutants was obtained by molecular replacement using the VrEH2<sub>M263N</sub> (PDB ID: **5Y6Y**) as search template. Then the structure was refined by the software Phenix<sup>[20]</sup> and the collected data and refinement result are listed in **Table S4**. The molecular docking was carried out using the software AutodockingTools 1.5.6,<sup>[21]</sup> the substrates were docked into the active site of WT and variants, respectively. The coordinate of central grid was determined based on the locations of the catalytic residues. The programs Autogrid 4 and Autodock 4 were performed by default.

## Acknowledgements

This work was financially supported by The National Key Research and Development Program of China (2019YFA09005000), The National Natural Science Foundation of China (21922804 & 21672063 & 21536004 & 21871085), and the Fundamental Research Funds for the Central Universities (22221818014); We are very grateful for the access to beamline BL17U1 at Shanghai Synchrotron Radiation Facility and thank the beamline staff for technical help. We also thank Simon Partridge, PhD, for editing the English text of a draft of this manuscript.

## References

- [1] a) A. Archelas, R. Furstoss, *Curr. Opin. Chem. Biol.* **2001**, *5*, 112-119; b) N. Bala, S. S. Chimni, *Tetrahedron: Asymmetry* **2010**, *21*, 2879-2898; c) M. Kotik, A. Archelas, R. Wohlgemuth, *Curr. Org. Chem.* **2012**, *16*, 451-482.
- [2] a) Y. Nie, Y. Xu, M. X. Yang, Q. Mu, *Lett. Appl. Microbiol.* **2007**, *44*, 555-562; b) R. Kadyrov, R. M. Koenigs, C. Brinkmann, D. Voigtlaender, M. Rueping, *Angew. Chem. Int. Ed.* **2009**, *48*, 7556-7559; c) A. Li, J. Liu, S. Q. Pham, Z. Li, *Chem. Commun.* **2013**, *49*, 11572-11574.
- [3] Y. Nie, Y. Xu, M. Yang, X. Q. Mu, *Lett. Appl. Microbiol.* **2010**, *44*, 555-562.
- [4] a) S. Pedragosa-Moreau, C. Morisseau, J. Zylber, A. Archelas, J. Baratti, R. Furstoss, *J. Org. Chem.* **1996**, *61*, 7402-7407; b) G. Bellucci, C. Chiappe, A. Cordoni, *Tetrahedron: Asymmetry* **1996**, *7*, 197-202; c) Y. Genzel, A. Archelas, J. H. L. Spelberg, D. B. Janssen, R. Furstoss, *Tetrahedron*, **2001**, *57*, 2775-2779; d) N. Bala, S. S. Chimni, H. S. Saini, B. S. Chadha, *J. Mol. Catal. B-Enzym.* **2010**, *63*, 128-134; e) J. T. Mohr, J. T. Moore, B. M. Stoltz, *Beilstein J. Org. Chem.* **2016**, *12*, 2038-2045.
- [5] a) G. Bellucci, C. Chiappe, A. Cordoni, *Tetrahedron: Asymmetry* **1996**, *7*, 197-202; b) A. Steinreiber, S. F. Mayer, R. Saf, K. Faber, *Tetrahedron: Asymmetry* **2001**, *12*, 1519-1528.
- [6] M. I. Monterde, M. Lombard, A. Archelas, A. Cronin, M. Arand, R. Furstoss, *Tetrahedron: Asymmetry* **2004**, *15*, 2801-2805.
- [7] a) W. Xu, J. H. Xu, J. Pan, Q. Gu, X. Y. Wu, *Org. Lett.* **2006**, *8*, 1737-1740; b) Y. W. Wu, X. D. Kong, Q. Q. Zhu, L. Q. Fan, J. H. Xu, *Catal. Commun.* **2015**, *58*, 16-20; c) S. Hwang, C. Y. Choi, E. Y. Lee, *Biotechnol. Lett.* **2008**, *30*, 1219-1225; d) M. Kotik, V. Stepanek, M. Grulich, P. Kyslik, A. Archelas, *J. Mol. Catal. B-Enzym.* **2010**, *65*, 41-48; e) H. H. Ye, D. Hu, X. L. Shi, M. C. Wu, C. Deng, J. F. Li, *Catal. Commun.* **2016**, *87*, 32-35; f) B. C. Hu, C. Li, R. Wang, X. C. Zong, J. Li, J. F. Li, M. C. Wu, *Catal. Commun.* **2018**, *117*, 9-13; g) C. Li, J. Zhao, D. Hu, B. C. Hu, R. Wang, J. Zang, M. C. Wu, *Int. J. Biol. Macromol.* **2019**, *121*, 326-332.
- [8] a) L. K. Morlock, S. Grobe, K. Balke, S. Mauersberger, D. Boettcher, U. T. Bornscheuer, *ChemBioChem* **2018**, *19*, 1954-1958; b) M. C. Andorfer, H. J. Park, J. Vergara-Coll, J. C. Lewis, *Chem. Sci.* **2016**, *7*, 3720-3729; c) C. G. Acevedo-Rocha, C. G. Gamble, R. Lonsdale, A. Li, N. Nett, S. Hoebenreich, J. B. Lingnau, C. Wirtz, C. Fares, H. Hinrichs, A. Deege, A. J. Mulholland, Y. Nov, D. Leys, K. J. McLean, A. W. Munro, M. T. Reetz, *ACS Catal.* **2018**, *8*, 3395-3410; d) C. G. Acevedo-Rocha, M. Ferla, M. T. Reetz, *Methods Mol. Biol.* **2018**, *1685*, 87-128; e) M. C. C. J. C. Ebert, J. G. Espinola, G. Lamoureux, J. N. Pelletier, *ACS Catal.* **2017**, *7*, 6786-6797; f) M. Kotik, W. Zhao, G. Iacazio, A. Archelas, *J. Mol. Catal. B-Enzym.* **2013**, *91*, 44-51.
- [9] F. L. Li, X. D. Kong, Q. Chen, Y. C. Zheng, Q. Xu, F. F. Chen, L. Q. Fan, G. Q. Lin, J. Zhou, H. L. Yu, J. H. Xu, *ACS Catal.* **2018**, *8*, 8314-8317.
- [10] D. Hu, X. Zong, F. Xue, C. Li, B. C. Hu, M. C. Wu, *Chem Commun.* **2020**, *56*, 2799-2802.
- [11] a) M. T. Reetz, M. Bocola, J. D. Carballeira, D. Zha, A. Vogel, **2005**, *44*, 4192-4196. b) Q. Wu, P. Soni, M. T. Reetz, *J. Am. Chem. Soc.* **2013**, *135*, 1872-1881. c) Z. Sun, R. Lonsdale; X. D. Kong, J. H. Xu, J. Zhou, M. T. Reetz, *Angew. Chem., Int. Ed.* **2015**, *54*, 12410-12415. d) Z. Sun, P. T. Salas, E. Siirola, R. Lonsdale, M. T. Reetz, *Bioresour. Bioprocess.* **2016**, *3*, 44. e) G. Qu, A. Li, C. G. Acevedo-Rocha, Z. Sun, M. T. Reetz, *Angew. Chem. Int. Ed.* **2020**, *59*, 13204-13231; f) H. Fujii, X. Zhang, T. Yoshida, *J. Am. Chem. Soc.* **2004**, *126*, 4466-4467; g) J. Bendl, J. Stourac, E. Sebestova, O. Vavra, M. Musil, J. Brezovsky, J. Damborsky, *Nucleic Acids Res.* **2016**, *44*, W479-487; h) X. D. Kong, Q. Ma, J. Zhou, B. B. Zeng, J. H. Xu, *Angew. Chem., Int. Ed.* **2014**, *53*, 6641-6644; i) K. Balke, S. Schmidt, M. Genz, U. T. Bornscheuer, *ACS Chem. Bio.* **2016**, *11*, 38-43; k) X. Chen, H. Zhang, J. Feng, Q. Wu, D. Zhu, *ACS Catal.* **2018**, *8*, 3525-3531.
- [12] a) E. J. Corey, J. O. Link, *J. Org. Chem.* **1991**, *56*, 442-444; b) F. E. Held, S. Wei, K. Eder, S. B. Tsogoeva, *RSC Advances* **2014**, *4*, 32796-32801; c) R. Hertzberg, G. Monreal Santiago, C. Moberg, *J. Org. Chem.* **2015**, *80*, 2937-2941; d) S. Wei, R. Messerer, S. B. Tsogoeva, *Chem. Eur. J.* **2011**, *17*, 14380-14384.
- [13] a) R. Kadyrov, R. M. Koenigs, C. Brinkmann, D. Voigtlaender, M. Rueping, *Angew. Chem. Int. Ed.* **2009**, *48*, 7556-7559. b) S. E. Schaus, B. D. Brandes, J. F. Larrow, M. Tokunaga, K. B. Hansen, A. E. Gould, M. E. Furrow, E. N. Jacobsen, *J. Am. Chem. Soc.* **2002**, *124*, 1307-1315.
- [14] P. Moussou, A. Archelas, J. Baratti, R. Furstoss, *Tetrahedron: Asymmetry* **1998**, *9*, 1539-1547.
- [15] T. Ohkuma, N. Utsumi, M. Watanabe, K. Tsutsumi, N. Arai, K. Murata, *Org. Lett.* **2007**, *9*, 2565-2567.
- [16] R. Kadyrov, R. M. Koenigs, C. Brinkmann, D. Voigtlaender, M. Rueping, *Angew. Chem. Int. Ed.* **2009**, *48*, 7556-7559.
- [17] Q. S. Wang, K. H. Zhang, Y. Cui, Z. J. Wang, Q. Y. Pan, K. Liu, B. Sun, H. Zhou, M. J. Li, Q. Xu, C. Y. Xu, F. Yu, J. H. He, *Nucl. Sci. Tech.* **2018**, *29*, 68.
- [18] Z. Otwinowski, W. Minor, *Methods Enzymol.* **1997**, *276*, 307-326.

- [20] a) A. J. McCoy, K. R. W. Grosse, P. D. Adams, M. D. Winn, L. C. Storoni, R. J. Read, *J. Appl. Crystallogr.* **2007**, *40*, 658-674.  
b) P. D. Adams, P. V. Afonine, G. Bunkoczi, V. B. Chen, I. W. Davis, N. Echols, J. J. Headd, L. W. Hung, G. J. Kapral, R. W. Grosse-Kunstleve, A. J. McCoy, N. W. Moriarty, R. Oeffner, R. J. Read, D. C. Richardson, J. S. Richardson, T. C. Terwilliger, P. H. Zwart, *Acta. Crystallogr. D. Biol. Crystallogr.* **2010**, *66*, 213-221.
- [21] G. M. Morris, R. Huey, W. Lindstrom, M. F. Sanner, R. K. Belew, D. S. Goodsell, A. J. Olson, *J. Comput. Chem.* **2009**, *30*, 2785-2791.

## FULL PAPER

**Reprogramming Epoxide Hydrolase to Improve Enantioconvergence in Hydrolysis of Styrene Oxide Scaffolds**

*Adv. Synth. Catal.* 2020 Volume, Page – Page

Fu-Long Li, Yan-Yan Qiu, Yu-Cong Zheng, Fei-Fei Chen, Xu-Dong Kong, Jian-He Xu\* and Hui-Lei Yu\*

